Ultrastructure, Pharmacologic Inhibition, and Transport Selectivity of Aquaporin Channel-Forming Integral Protein in Proteoliposomes†

Mark L. Zeidel,‡ Søren Nielsen,§ Barbara L. Smith,∥,⊥ Suresh V. Ambudkar,∥,# Arvid B. Maunsbach,§ and Peter Agre*,∥,⊥

Renal-Electrolyte Division, University of Pittsburgh School of Medicine, Room F1159, Presbyterian University Hospital, Pittsburgh, Pennsylvania 15261, Departments of Medicine, Biological Chemistry, and Physiology, Johns Hopkins University School of Medicine, Baltimore, Maryland 21205, and Department of Cell Biology, Institute of Anatomy, University of Aarhus, DK-8000 Aarhus C, Denmark

Received August 18, 1993; Revised Manuscript Received October 15, 1993®

ABSTRACT: Reconstitution of highly purified aquaporin CHIP (channel-forming integral protein) into proteoliposomes was previously shown to confer high osmotic water permeability (P_f) to the membranes [Zeidel et al. (1992) *Biochemistry 31*, 7436–7440]. Here we report detailed ultrastructural, pharmacologic, and transport studies of human red cell CHIP in proteoliposomes. Freeze–fracture and transmission electron microscopy revealed a uniform distribution of CHIP which was incorporated into the membranes in both native and inverse orientations. Morphometric analysis of membranes reconstituted at three different concentrations of CHIP revealed that the intramembrane particles correspond to tetramers or possible higher order oligomers, and the P_f increased in direct proportion to the CHIP density. Proteolytic removal of the 4-kDa C-terminal cytoplasmic domain of CHIP did not alter the P_f or oligomerization in red cell membranes. CHIP exhibited a similar conductance for water when reconstituted into membranes of varied lipid compositions. The sensitivities of CHIP-mediated P_f to specific sulfhydryl reagents were identical to known sensitivities of red cell P_f, including a delayed response to *p*-(chloromercuri)benzenesulfonate. CHIP did not increase the permeability of the proteoliposome membranes to H^+/OH^- or NH_3. These studies demonstrate that CHIP proteoliposomes exhibit all known characteristics of water channels in native red cells and therefore provide a defined system for biophysical analysis of transmembrane water movements.

Because water crosses the lipid bilayer of most cell membranes slowly, water flux occurs in certain cell types through specialized water-selective channels. These channels permit rapid cell swelling and shrinkage in response to small changes in extracellular osmolality, and mediate water reabsorption by ADH-responsive cells (e.g. mammalian renal collecting ducts) and unresponsive cells (e.g. mammalian red cells and renal proximal tubules) (Finkelstein, 1987; Verkman, 1989; Macey, 1984; Harris et al., 1991). Extensive biophysical studies have established that water channels in native cell membranes are inhibited by organic mercurial reagents such as pCMBS[1] and $HgCl_2$, and exhibit activation energies (E_a) of <5 kcal/mol, a value similar to that of isotopic water diffusing through aqueous solutions (Finkelstein, 1987; Macey, 1984). Despite intensive efforts, the molecular water channel eluded identification until recently.

Aquaporin CHIP is a 28-kDa integral membrane protein, and several lines of evidence indicate that CHIP is a constitutively active membrane water channel. CHIP is abundant in mammalian red cells, renal proximal tubules (Denker et al., 1988; Smith & Agre, 1991), and other water-permeable epithelia (Nielsen et al., 1993a,b). The total number of CHIP monomers in a human red cell (2×10^5) is similar to the number of water channels estimated from biophysical analyses (2.7×10^5; Finkelstein, 1987). The 28.5-kDa molecular size of the CHIP monomer is similar to the 30 kDa functional unit of proximal tubule water channels as revealed by radiation inactivation studies (van Hoek, et al., 1991). The CHIP cDNA encodes a channel-like protein with six membrane-spanning domains (Preston & Agre, 1991), and is the product of a single gene located at 7p14 in the human genome (Moon et al., 1993). Expression of CHIP in *Xenopus laevis* oocytes confers a markedly increased osmotic water permeability coefficient which is inhibited by $HgCl_2$ and exhibits an activation energy < 3 kcal/mol (Preston et al., 1992). Reconstitution of pure CHIP into proteoliposomes demonstrated that the protein is both necessary and sufficient to confer enhanced osmotic water permeability (P_f) (Zeidel et al., 1992b). Several of these studies have been confirmed and further defined by others (Van Hoek & Verkman, 1992; Sabolic et al., 1992; Zhang et al., 1993; Echevarria et al., 1993). Moreover, other water conducting proteins homologous to CHIP have been recognized in plants (Maurel et al., 1993) and mammals (Fushimi et al., 1993), and this group of proteins is now referred to as the Aquaporins (Agre et al., 1993).

Several aspects of the function of CHIP proteoliposomes remain unclear. These include the structural organization of

† Supported by NIH Grants DK43955, HL33991, HL48268, and CA 57154, American Cancer Society Grant BE157, the Danish Medical Research Council, the Biomembrane Research Center and Foundation of the University of Aarhus, and the Novo Foundation. M.L.Z. is the recipient of a Career Development Award from the Department of Veterans Affairs.

* Author to whom correspondence should be addressed at the Department of Biological Chemistry, Johns Hopkins University School of Medicine, 725 N. Wolfe Street, Baltimore, MD 21205-2185.

‡ Presbyterian University Hospital.

§ University of Aarhus.

∥ Department of Medicine, Johns Hopkins University of School of Medicine.

⊥ Department of Biological Chemistry, Johns Hopkins University School of Medicine.

Department of Physiology, Johns Hopkins University School of Medicine.

® Abstract published in *Advance ACS Abstracts,* February 1, 1994.

[1] Abbreviations: CHIP, channel-forming integral protein of 28 kDa; FMA, fluorescein mercuric acetate; CF, 5(and 6)-carboxyfluorescein; pCMBS, *p*-(chloromercuri)benzenesulfonate; PMSF, toluenesulfonyl fluoride.

0006-2960/94/0433-1606$04.50/0

reconstituted CHIP, the role that structural domains of the protein play in water channel function, the role of membrane lipids in water channel function, the selective mercurial sensitivities of the molecule, and the selectivity of the channel to small molecules such as H^+ and NH_3. The present studies were designed to approach these questions by examining the function of pure CHIP reconstituted into proteoliposomes.

MATERIALS AND METHODS

Materials. Octyl β-D-glucopyranoside was obtained from Calbiochem. Triton X-100, dithiothreitol, PMSF, and *N*-lauroylsarcosine were from Sigma. CF was from Molecular Probes, Junction City, OR. Anti-fluorescein antibody was prepared as described (Harris et al., 1990). Crude *Escherichia coli* lipid and other phospholipids were from Avanti Polar Lipids, Inc., and neutral lipid was removed by acetone/ether wash (Ambudkar and Maloney, 1986a). The purified *E. coli* bulk phospholipid is composed of phosphatidylethanolamine (70%), phosphatidylglycerol (15%), and cardiolipin (15%) (Chen & Wilson, 1984). α-Chymotrypsin was obtained from Cooper Biomedical. Anticoagulated normal human blood was obtained from the American Red Cross.

Purification of CHIP Protein. CHIP purification methods were adapted from our published study (Smith & Agre, 1991). KI-stripped red cell membrane vesicles from 900 mL of human blood were extracted with 1% (w/v) *N*-lauroylsarcosine and solubilized in 4% Triton X-100 (v/v) as described (Nielsen et al., 1993a). The solubilized material was filtered through a 0.22-μm Millipore Sterifil D-GV apparatus. A 600-mL aliquot of the filtrate (corresponding to 200 mL of packed membranes) was loaded onto a 10 mm × 100 mm POROS Q/F column (PerSeptive Biosystems, Cambridge, MA) equilibrated with 0.1% Triton X-100, 20 mM Tris-HCl (pH 7.8), 1 mM NaN_3, 1 mM dithiothreitol driven at 3 mL/min by a Pharmacia FPLC apparatus. The column was washed with 40 mL of equilibrium buffer and eluted with a 120-mL 0.2–0.6 M NaCl gradient at 4 mL/min while A_{280} was monitored. Peaks eluted at 0.35 M NaCl, and fractions from two runs were combined, diluted to six volumes with 1.2% octyl glucopyranoside, 20 mM Tris-HCl (pH 7.8), 1 mM NaN_3, 1 mM dithiothreitol, and loaded onto the same POROS column equilibrated with the same buffer while running at 2 mL/min. The column was washed until the A_{280} baseline was recovered, and then eluted at 1 mL/min with a 40-mL gradient of 0–0.6 M NaCl in the same buffer. The combined peak fractions, eluted at 0.25 M NaCl, contained pure aquaporin CHIP at 630 μg/mL (BCA protein method, Pierce, Rockford, IL), and were snap frozen and stored at −80 °C until reconstitution.

Reconstitution into Proteoliposomes. Reconstitution was carried out in a final volume of 1 mL containing 60–90 μg of purified CHIP protein in chromatography buffer, 9 mg of bath-sonicated *E. coli* phospholipid, 1.25% (w/v) octyl glucopyranoside, and 50 mM Tris-HCl (pH 7.5). In certain experiments, other lipids were included (Zeidel et al., 1992b). The mixture was briefly blended on a vortex mixer and incubated for 20 min on ice. Proteoliposomes (or liposomes prepared without protein) were formed at room temperature by rapidly injecting the mixture into 25 mL of buffer A [50 mM MOPS, pH 7.5, 150 mM *N*-methyl-D-glucamine (NMDG) chloride also containing 10–15 mM CF, 1 mM dithiothreitol, and 0.5 mM PMSF]. For the measurement of proton permeability, proteoliposomes and liposomes were loaded with buffer B (5 mM MOPS, pH 7.5, 150 mM KCl, 0.5 mM CF, 1 mM dithiothreitol, and 0.5 mM PMSF). The suspension was incubated for 20 min at room temperature. Proteoliposomes or liposomes were collected by centrifugation for 1 h at 123000*g* in a Beckman Type 42.1 rotor at 4 °C. The pellet was resuspended in 8 mL of buffer A or B and then centrifuged for 1 h at 152000*g* in a Beckman Type 50 Ti rotor. Proteoliposomes or liposomes were resuspended in 300 μL of buffer A or B and stored at 4 °C for 16–24 h. Typically 50% (54 ± 6%, $n = 5$) of the CHIP protein and 70% of the phospholipid were recovered in proteoliposomes. The lipid to protein ratio was in the range of 125:1 to 25:1. These proteoliposomes have internal volumes of 1 μL/mg phospholipid (Ambudkar & Maloney, 1986b). Protein and phospholipid were measured as described (Ambudkar & Maloney, 1986b).

Electron Microscopy Analysis of Proteoliposomes. General methods were described previously (Maunsbach et al., 1988; Skriver et al., 1980). Pellets of freshly prepared liposomes and proteoliposomes containing CHIP reconstituted at different densities were prepared by centrifugation at 100 000 rpm for 2 min at 20 °C in a Beckman airfuge.

Freeze–fracture was performed by resuspending the pellets in glycerol to a final concentration of 20% in buffer and equilibrating for 1–3 h on ice. Liposome aliquots were placed on gold holders and snap frozen in Freon 22 cooled by liquid nitrogen. Specimens were fractured in a Balzer's freeze–fracture apparatus (BAF 300, Balzers AG, Lichtenstein) at −100 °C. They were shadowed immediately at an angle of 45° or rotary shadowed at 15°, both with platinum, before being replicated with carbon. After being cleaned with hypochlorite, the replicas were analyzed with a JEOL 100 CX or Zeiss 902 electron microscope.

Morphometric analysis of freeze-fractured proteoliposomes was performed on random micrographs taken within regions of the replica with a shadowing angle at 45°. Micrographs were taken at an initial magnification of 33000×, and enlarged to a final magnification of 100000×. Calibration was performed using carbon grating replicas (2160 lines/mm). Diameters were determined on micrographs where the fracture plane corresponded to the equatorial plane of the individual liposomes or proteoliposome. The diameter of both concave and convex fractures were measured at right angles to the direction of shadowing. Particle densities were determined on liposomes fractured in planes distinct from the equatorial plane to obtain an area in the center of the proteoliposome with optimal visibility of the particles. A test circle (0.8 mm in diameter) with two steering lines was placed in the center of all convex and all concave fracture faces having the edge of the platinum shadow outside the test circle. Particles that were enclosed by the circle, plus the particles intersecting with the upper half of the test circle, were counted.

Freeze substitution of proteoliposomes and immunolabeling was performed on aliquots of liposomes cryoprotected with 20% glycerol placed in 1% agarose, mounted on holders, and snap frozen in liquid nitrogen. Samples were freeze-substituted (Maunsbach & Reinholt, 1992) in Balzers freeze-substitution unit (FSU 010, Balzers AG, Lichtenstein). Briefly, the samples were sequentially equilibrated over 3 days in 0.5% uranyl acetate in methanol at temperatures gradually decreasing from −90 to −70 °C, and then in pure methanol for 24 h at −70 to −45 °C. At 45 °C the samples were equilibrated with Lowicryl HM20 and methanol 1:1 and 2:1 and finally pure HM20 before UV polymerization for 2 days at −40 °C and 2 days at 0 °C.

Ultrathin sections were incubated with affinity-purified anti-CHIP antibody (0.07 μg/mL) specific for the 4-kDa C-terminus of the protein (Smith & Agre, 1991) and visualized

with protein-A gold (Nielsen et al., 1993a,b). Specificity of immunolabeling was confirmed with nonimmune rabbit IgG. Negative staining was performed on resuspended liposomes with either 1% uranyl acetate, aurothiosulfate, or glucose for 1 min subsequent to immunolabeling using the same labeling conditions as described for ultrathin sections (see above).

Chymotrypsin Digestions of CHIP. Red cell membranes were prepared by hypotonic lysis followed by extraction of all peripheral membrane proteins with KI (Bennett, 1983). The membranes were suspended to 1 mg total protein/mL in 7.5 mM sodium phosphate (pH 7.4) which was equivalent to approximately 50 μg of CHIP/mL. CHIP proteoliposomes were suspended similarly to approximately 14 μg of CHIP/mL. α-Chymotrypsin (45 units/mg) was added to 10 μg/mL of suspension and incubated for 1 h at 37 °C. Control digestions were performed similarly but without enzyme. PMSF was added to 4 mM final concentration, and SDS–PAGE samples were prepared and analyzed by SDS–PAGE immunoblot. In other experiments, the digests were solubilized in 4% Triton X-100 and analyzed by velocity sedimentation through 5–20% sucrose gradients (Smith & Agre, 1991).

Membrane Permeability Measurements. For measurements of P_f, CHIP proteoliposomes, control liposomes, or inside-out red cell membranes were loaded with 10 mM CF by overnight incubation, followed by removal of excess extravesicular CF by centrifugation immediately prior to use. For measurements of P_{H^+} or P_{NH_3}, vesicles were incubated overnight in 0.5 mM CF (Priver et al., 1993). P_f was measured as described (Zeidel et al., 1992b) by abruptly exposing vesicles to a 20% increase in extravesicular osmolality using a stopped-flow fluorimeter (SF.17MV, Applied Photophysics, Leatherhead, UK) with a measured dead time of 0.7 ms. Excitation wavelength was 490 ± 1.5 nm, using a monochrometer, and emission wavelength was >515 nm, using a cut-on filter (Oriel Corp., Stratford, CT). Extravesicular CF fluorescence was completely quenched using anti-fluorescein antibody (Harris et al., 1990). Vesicles acted as perfect osmometers, and relative volume (absolute volume divided by initial volume) was linearly related to relative fluorescence (absolute fluorescence divided by initial fluorescence). Data obtained from 8 to 16 determinations was averaged and fit to single exponential curves using software provided by Applied Photophysics (Zeidel et al., 1992a,b). Fitting parameters were then used to determine P_f exactly as described (Priver et al., 1993; Zeidel et al., 1992a,b).

The radii of membranes were measured by electron microscopy and averaged 7.0 ± 0.7 × 10^{-6} cm for liposomes and proteoliposomes, and 2.6 ± 0.2 × 10^{-5} cm for inside-out red cell membranes. The number of CHIP molecules/mL of suspension was calculated from the amount of protein/mL in each preparation and the molecular weight of CHIP (28 500 Da). The measured total entrapped volume/mg of phospholipid, the calculated volume of each liposome, and the total number of liposomes/mL of suspension were calculated from the total phospholipid content. Dividing the number of protein molecules/mL of suspension by the number of proteoliposomes/mL of suspension gave the numbers of protein molecules/proteoliposome.

Proton permeability was measured in vesicles containing 150 mM KCl and 5 mM MOPS, incorporating 1 μM valinomycin to prevent accumulation of protons from generating a positive intravesicular voltage (Harris et al., 1990; Priver et al., 1993). Vesicles at pH 7.40 were abruptly exposed to a solution of pH 6.80 and the time course of the fall in intravesicular pH was followed on the stopped-flow device by monitoring the quenching by protons of 0.5 mM entrapped CF. Over the pH range employed, fluorescence was linearly related to pH; extravesicular fluorescence was quenched with anti-fluorescein antibody. To insure that increases in P_{H^+} caused by CHIP could have been detected, 1 μM gramicidin A was added and increased P_{H^+} by over 50-fold in each experiment. The ethanol vehicle used for the valinomycin and gramicidin did not alter the high P_f of CHIP proteoliposomes.

NH_3 permeability (P_{NH_3}) was determined by rapid mixing of the vesicles at pH 6.8 with ammonium chloride at a final concentration of 20 mM (Priver et al., 1993). Under these conditions, the small amount of NH_3 present in the ammonium chloride rapidly permeates the membrane. Upon entering the vesicle, the NH_3 titrates a proton, forming NH_4^+ and raising the intravesicular pH (Roos & Boron, 1981). The final intracellular pH was determined from the linear correlation between relative fluorescence and pH. Using the rate of change in intravesicular pH and the calculated buffer capacity, P_{NH_3} was calculated.

RESULTS

Ultrastructural Analysis of CHIP Proteoliposomes. Freeze–fracture of proteoliposomes reconstituted with CHIP showed uniform populations of concave and convex fracture faces (Figure 1A), and the ratio between the total number of convex and concave fracture faces was close to unity in each preparation. Vesicle diameters were also similar in each preparation and were not altered by variation in the density of CHIP (Table 1). Intramembrane particles were not observed in liposomes reconstituted without CHIP (Figure 1B), whereas proteoliposomes reconstituted with CHIP showed distinct intramembrane particles with a uniform appearance (Figure 1C–G). High magnification electron microscopy of unidirectional or rotary shadowed proteoliposome fracture faces (Figure 1F,G) permitted determination of the average particle diameter (8.5–9.5 nm), but no distinct substructure was observed.

CHIP proteoliposomes contained particles which were distributed equally on the convex and concave fracture faces (Figure 1 and Table 1), with particles being evenly distributed on both faces. Morphometric determination of particle frequencies revealed an increased number of particles in proteoliposomes containing higher concentrations of CHIP, as determined by protein and lipid assays (Table 1). The total number of particles/liposome was determined from the number of particles/μm^2 membrane by using the average diameter of the liposomes. The number of CHIP molecules expressed in relation to the number of intramembrane particles/liposome, was 4.4 when CHIP was reconstituted at a density equivalent to that of the red cell. When reconstituted at higher densities, the ratio of CHIP/IMP increased somewhat, suggesting that CHIP may reach higher oligomerization levels.

Unstained and negatively stained proteoliposome preparations were subjected to immunolabeling with affinity purified anti-CHIP IgG (Figure 2). The immunolabeling was evenly distributed over CHIP proteoliposomes (Figure 2A,B), whereas control liposomes showed no labeling (Figure 2C). Ultrathin sections of densely packed, cryosubstituted CHIP proteoliposomes permitted semiquantitative analysis of the sidedness of the distribution of gold particles, although some vesicles had been compressed or invaginated during preparation (Figure 2D,E). Of 304 particles counted, 41% were associated with the inside, 40% associated with the outside, and 19%

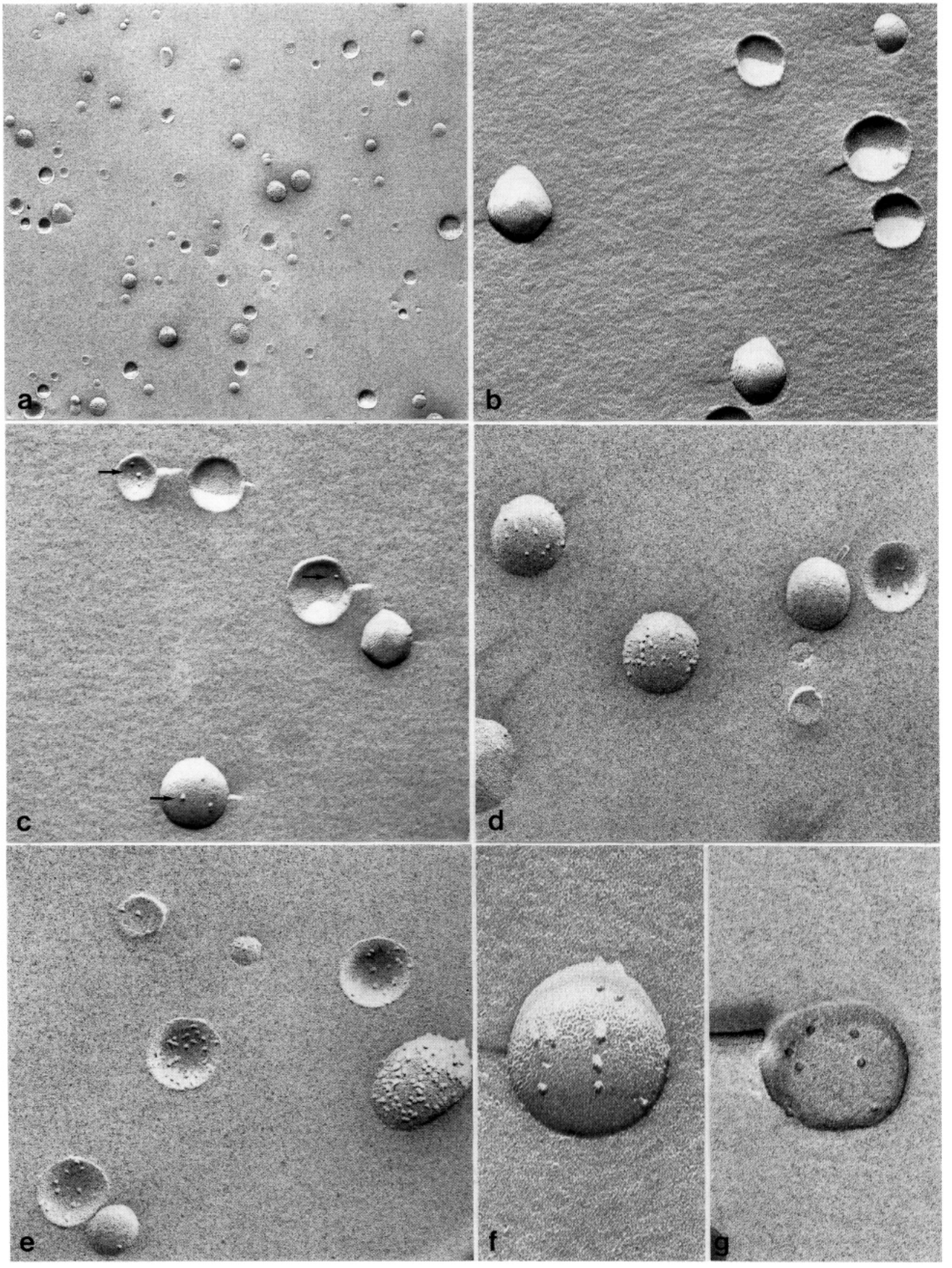

FIGURE 1: Electron micrographs (shown at 95% of original size) of freeze–fracture replicas of control liposomes and proteoliposomes reconstituted at 1×, 2.5×, and 5× the red cell CHIP concentration (see Table 1). (A) Survey electron micrograph of freeze–fracture replica of proteoliposomes showing the uniform populations of vesicles (18000×). (B) Control liposomes exhibit no intramembrane particles (90000×). (C–E) Proteoliposomes reconstituted with increasing concentrations of CHIP exhibit increasing particle densities (C = 1× CHIP; D = 2.5×; E = 5×)(90000×). (F) Unidirectional shadowing at a 45° angle of a freeze–fracture replica of CHIP proteoliposomes reveals uniform distribution of intramembrane particles (200000×). (G) Rotary shadowing at 15° reveals symmetric intramembrane particles without distinct substructures (200000×).

Table 1: Intramembrane Particle (IMP) Density in CHIP Proteoliposomes

preparation[a]	proteoliposome diameter, μm	no. IMP[b]	IMP/ μm²	CHIP/ proteoliposome[c]	CHIP/ IMP
control	nd	0	0	0	0
1×	0.147 ± 0.003 (n = 32)	724	536	146	4.4
2.5×	0.148 ± 0.009 (n = 68)	1634	1191	465	6.3
5×	0.153 ± 0.003 (n = 77)	1310	1762	760	7.0

[a] Refers to approximate increase in CHIP density in proteoliposomes compared to normal red cell membranes. [b] Refers to total number of IMP counted in ≥500 test areas (see Methods and Materials). [c] Refers to the number of 28-kDa subunits as determined by protein and lipid analyses (see Methods and Materials).

localized directly over the membrane. Freeze–fracture analysis of dispersed proteoliposomes revealed the presence of only very rare multilamellar vesicles (<1%, Figure 1).

Water Conductance of CHIP Proteoliposomes. On the basis of measurements in proteoliposomes containing CHIP at one concentration, it was previously reported that CHIP exhibits a unit water conductance (p_f) of 11.7 ± 1.8 × 10^{-14} cm^3/s per CHIP subunit (Zeidel et al., 1992b). To determine this conductance more precisely, the concentration of CHIP in the proteoliposomes was varied and osmotic water permeabilities were measured. As shown in Figure 3, the P_F increased linearly with the density of CHIP, ranging from 0–760 CHIP subunits/proteoliposome. From the slope of the line, the CHIP conductance was calculated to be 4.6 × 10^{-14} cm^3/s per CHIP subunit (R = 0.976). Efforts to determine the diffusive water permeability of CHIP proteoliposomes using entrapped 8-aminonaphthalenetrisulfonic acid (ANTS) to monitor deuterium fluxes did not give reliable estimates (data not shown; Ye & Verkman, 1989).

Analysis of 24-kDa Chymotrypsin-Resistant Bilayer Spanning Domains of CHIP. It was previously demonstrated that the N- and C-terminal domains of CHIP are localized at the cytoplasmic face of the lipid bilayer, and the 4-kDa C-terminal domain may be removed by α-chymotrypsin digestion, leaving the N-terminal 24-kDa fragment within the bilayer (Smith & Agre, 1991). Therefore, the function of the C-terminal portion of the protein may be evaluated after α-chymotrypsin digestion of inside-out membranes. As shown in Figure 4A, exposure to α-chymotrypsin resulted in loss of the 4-kDa C-terminal domain from inside-out membranes. The molecular weight of the species reactive with the N-terminal antibody was decreased to approximately 24 kDa. A similar downward shift in the mobility of glyCHIP was detected with anti-N-peptide (faintly visible in Figure 4A). In contrast, CHIP proteoliposomes exposed similarly to α-chymotrypsin exhibited only partial digestion, with approximately half of the molecules remaining at 28 kDa and half undergoing cleavage to the 24-kDa fragment. Together with the electron

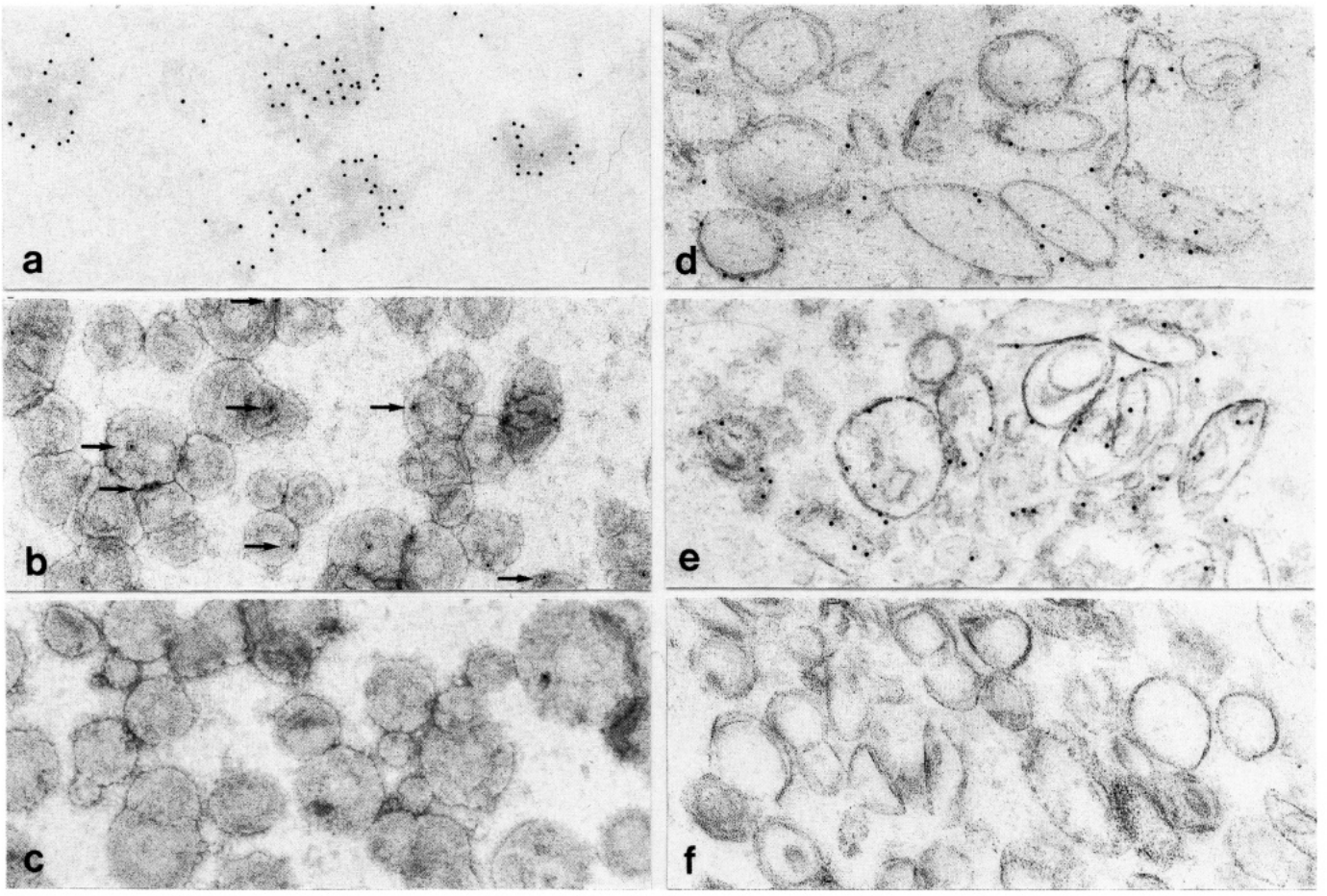

FIGURE 2: Anti-CHIP immunolabeling of unstained, negatively stained, and thin sections of freeze-substituted CHIP proteoliposomes. (A) Unstained glucose-embedded 5× CHIP proteoliposomes (see Table 1) show high density anti-CHIP immunolabeling which is evenly distributed over the membrane surface (46000×). (B) Uranyl acetate-stained 1× CHIP proteoliposomes show a uniform population with distinct anti-CHIP immunolabeling (46000×). (C) Incubation of 1× CHIP proteoliposomes with nonimmune IgG reveals no immunolabeling (46000×). (D,E) Different preparations of freeze-substituted proteoliposomes reconstituted with CHIP (D = 2.5× CHIP; E = 5×). The labeling is evenly distributed at both inner and outer surfaces of cross-sectioned proteoliposomes (60000×). (F) Freeze-substituted liposomes prepared without CHIP exhibit no labeling after incubation with anti-CHIP (60000×).

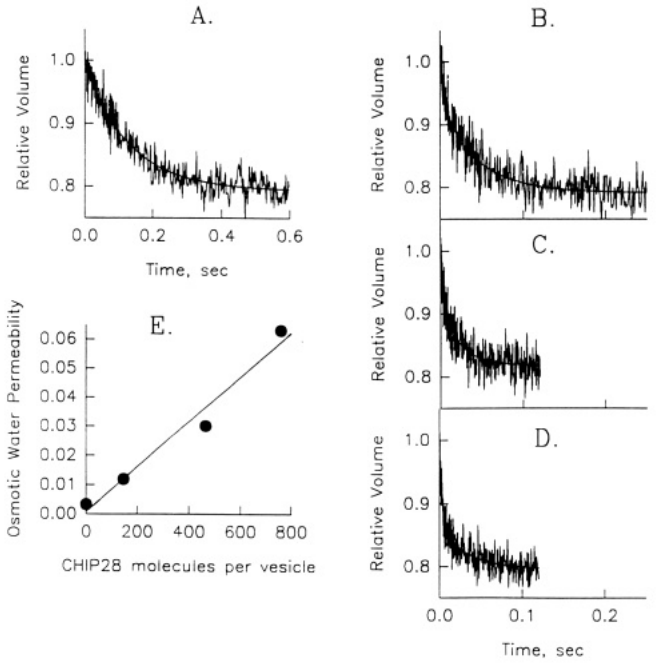

FIGURE 3: Effect of varying density of CHIP on osmotic water permeability of proteoliposomes. Control liposomes (A) and CHIP proteoliposomes (B = 1×; C = 2.5×; D = 5×) were subjected to an abrupt 20% increase in extravesicular osmolality on the stopped-flow device and water efflux was measured. (A-D) Fluorescence tracings and fitted curve are shown. (E) The measured P_f (ordinate, in cm/s) is plotted as a function of CHIP density (abscissa).

microscopy analyses, these studies indicate that CHIP is reconstituted into synthetic membranes in both orientations, with half of the molecules in the native orientation (exofacial domain outward) and half of the molecules inverted. Sedimentation analysis of α-chymotrypsin-degraded CHIP revealed S_w = 4.9, which is only slightly smaller than intact 28-kDa CHIP (Figure 4B), indicating that the 24-kDa fragment remains oligomeric.

Water permeability of inside-out red cell membranes was measured before and after α-chymotryptic digestion. As shown in Figure 5, water flux rates were similar in inside-out membranes containing 28-kDa CHIP and the α-chymotrypsin-cleaved 24-kDa protein. P_f averaged 0.018 ± 0.002 cm/s in control membranes and 0.018 ± 0.003 cm/s in membranes treated with α-chymotrypsin (n = 2). These values are similar to the P_f of intact red cells (0.02 cm/s; Finkelstein, 1987; Macey, 1984; Zeidel et al., 1992a). Moreover, the activation energies for water flow were identical in both preparations, averaging 4.7 ± 0.2 kcal/mol in each. Exposure to 1 mM $HgCl_2$ also gave similar responses, with P_f reduced to 0.0037 ± 0.0003 cm/s in control membranes and 0.0041 ± 0.0009 cm/s in chymotrypsin treated membranes, respectively.

CHIP Proteoliposomes with Varied Lipid Compositions. It is possible that water flux through channels occurs through a pore composed of both protein and lipid. To examine the role of lipid composition in CHIP-mediated P_f, the protein was reconstituted into proteoliposomes of varying lipid composition. Measurements of protein content and encapsulated volumes of the different preparations were similar. As shown in Table 2, addition of cholesterol to *E. coli* phospholipid and alteration of the phospholipid composition did not alter the behavior of CHIP proteoliposomes, including the permeability to water, sensitivity to $HgCl_2$, and activation energy.

Effects of Mercurial Reagents on CHIP Proteoliposomes. Water channels in intact red cells exhibit a characteristic response to different sulfhydryl reagents (see Benga, 1989).

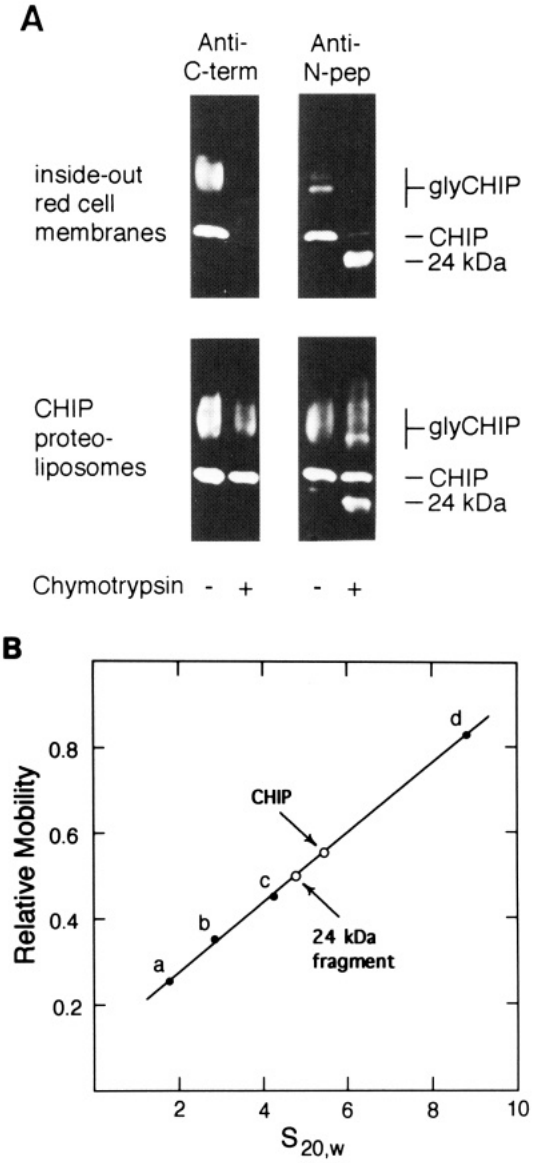

FIGURE 4: Orientation of CHIP in proteoliposomes and oligomeric state of a 24-kDa CHIP fragment. Inside-out red cell membranes and CHIP proteoliposomes were incubated with buffer or α-chymotrypsin, which cleaves the 4-kDa C-terminus of CHIP. (A) SDS–PAGE immunoblot analysis with anti-CHIP specific for C-terminus (Anti-C-term) or specific for N-terminus (Anti-N-pep) (Smith & Agre, 1991). Locations of glycosylated CHIP (glyCHIP), native 28-kDa CHIP (CHIP), and the 24-kDa CHIP fragment (24 kDa) on the gel are labeled. (B) Aliquots of Triton X-100-solubilized inside-out membranes from control (CHIP) and α-chymotrypsin-digested membranes (24-kDa fragment) analyzed by ultracentrifugation through 5–20% sucrose gradients relative to protein standards: (a) cytochrome c, 1.85; (b) carbonic anhydrase, 2.95; (c) bovine serum albumin, 4.35; and (d) β-amylase, 8.95.

$HgCl_2$ gives rapid, complete inhibition of water flow, while the response to pCMBS is complete, but delayed. FMA gives a partial inhibition, but NEM has no effect and does not alter the response to other mercurial reagents. Inhibition by mercurials is rapidly reversible with β-mercaptoethanol. To determine whether these effects can be accounted for by the CHIP molecule itself or are due to other properties of the red cell, the response of CHIP proteoliposomes to these reagents was examined (see Table 3). As is evident, the response of CHIP proteoliposomes to various sulfhydryl reagents was entirely similar to that observed in the intact red cells. Moreover, the time course of pCMBS inhibition of P_f at 37 °C was strikingly similar in CHIP proteoliposomes and intact

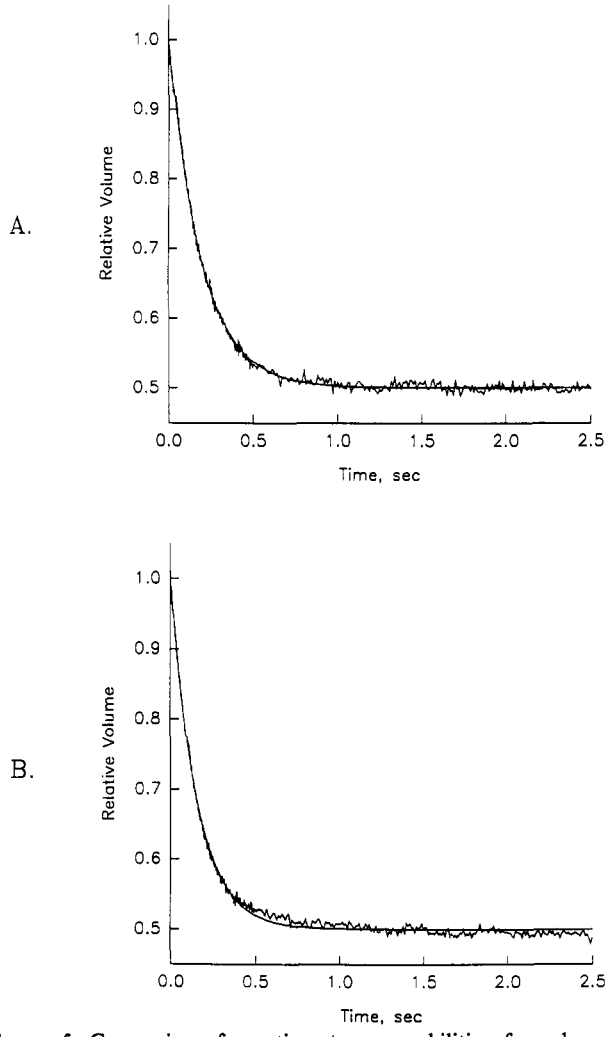

FIGURE 5: Comparison of osmotic water permeabilities of membranes containing 28-kDa CHIP or 24-kDa CHIP. Inside-out red cell membranes were abruptly exposed to a doubling of extravesicular osmolality, and the time course of water efflux was monitored on the stopped-flow device: (A) control membranes containing 28 kDa CHIP, (B) α-chymotrypsin-digested membranes containing 24-kDa CHIP.

Table 2: Effect of Lipid Composition on Water Flux in CHIP Proteoliposomes

lipid composition[b]	P_f, cm/s[a]	% $HgCl_2$ inhibition[a]	E_a, kcal/mol
E. coli phospholipids	0.012 ± 0.001	82 ± 3	3.2
E. coli phospholipids + 5% cholesterol	0.011 ± 0.004	80 ± 3	2.9
E. coli phospholipids + 15% cholesterol	0.011 ± 0.003	83 ± 1	4.7
E. coli phospholipids + 30% PC + 10% PS	0.012 ± 0.006	81 ± 4	2.8

[a] Mean ± SD of two preparations. [b] PC, phosphatidylcholine; PS, phosphatidylserine.

red cells (Figure 6). Cysteine-189 was previously shown to be the single residue in CHIP responsible for mercurial sensitivity (Preston et al., 1993). These results suggest that the slow time course of pCMBS inactivation results from the inaccessibility of the free sulfhydryl of Cys-189 to the reagent. Nevertheless, complete inhibition was achieved with pCMBS even though CHIP is reconstituted in these membranes in both orientations.

Transport Selectivity of CHIP Proteoliposomes. It was previously reported that CHIP proteoliposomes had markedly

Table 3: Inhibitor Sensitivities of Water Flux in CHIP Proteoliposomes and RBC

inhibitor	% decrease in RBC P_f[a]	% decrease in CHIP PL P_f
1 mM $HgCl_2$	90	87 ± 6
1 mM pCMBS	90	83 ± 8
1 mM NEM	<10	0 ± 0
0.5 mM FMA	45–50	70 ± 6
$HgCl_2$ + NEM	90	79 ± 5
$HgCl_2$ + β-ME	0	30 ± 9

[a] Data from Benga (1989).

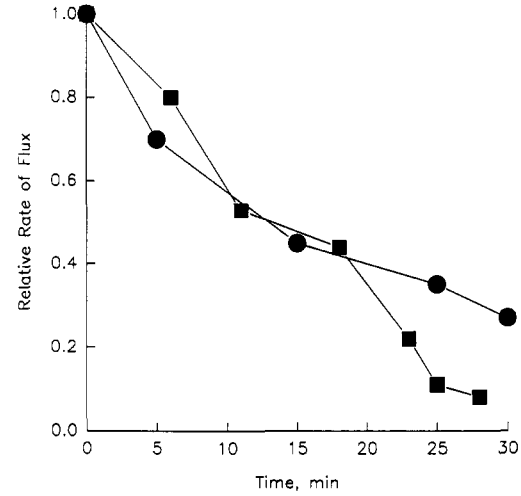

FIGURE 6: Time course of 1 mM pCMBS inhibition of P_f in 1× CHIP proteoliposomes (squares) and intact RBC (circles). Data for CHIP proteoliposomes is representative of similar determinations performed on three preparations. Data for intact red cells was taken from Macey (1984).

increased permeability to water, but not to urea (Zeidel et al, 1992b). To characterize further the selectivity of CHIP, we measured permeabilities to H^+ and NH_3. NH_3 and urea have molar volumes of 24.9 cm^3/mol and 45.5 cm^3/mol, as compared to a volume of 18 cm^3/mol for water. Figure 7 shows flux of H^+ across control liposomes (panel A) and CHIP proteoliposomes (panel B). No difference exists between control liposomes and CHIP proteoliposomes. In experiments using CHIP in sufficient density to increase P_f by 30-fold, we observed no increase in P_{H^+}. To insure that, under the experimental conditions, transmembrane flux of H^+ was rate-limiting, the flux measurement was repeated in proteoliposomes exposed to 1 μM levels of the proton and water pore gramicidin (panel C). As is evident, gramicidin increased P_{H^+} by more than 30-fold.

NH_3 has a molar volume similar to that of water. Although in equilibrium with NH_4^+, NH_3 is uncharged, and therefore may be a good index of the size selectivity of CHIP for water. As shown in Figure 8, P_{NH_3} was similar in the absence (panel A) or presence (panel B) of CHIP (both values averaged 0.012 ± 0.003 cm/s, SE; n = 4).

DISCUSSION

The recent recognition of aquaporin CHIP has made it possible to define the molecular mechanisms by which membranes conduct water. Studies of intact red cells had previously defined several characteristics of water channels in native membranes: high permeability to water but not to other small molecules (e.g., protons or urea), reversible inhibition by mercurial reagents, and low activation energy (Macey, 1984; Finkelstein, 1987; Verkman, 1989; Harris et al., 1991). Analyses of whole cell membranes are complicated

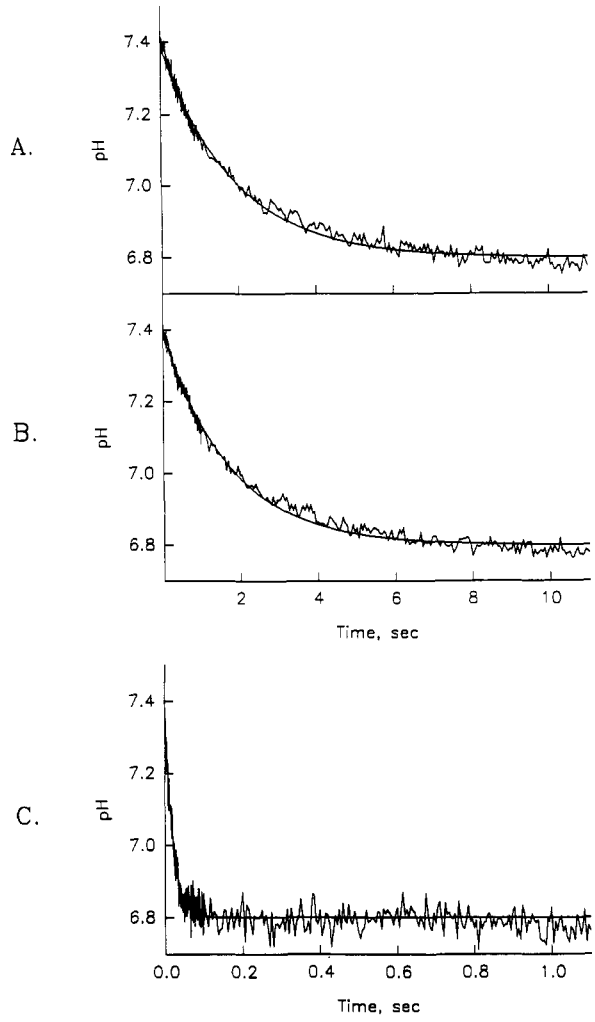

FIGURE 7: Comparison of proton flux into liposomes and CHIP proteoliposomes. Extravesicular pH was abruptly decreased from 7.4 to 6.8 and the time course of decline in intravesicular pH was recorded in the stopped-flow device. pH tracings are shown from control liposomes (A), 1× CHIP proteoliposomes (B), and 1× CHIP proteoliposomes exposed for 5 min to 1 μM gramicidin (C). Control liposomes exposed to gramicidin gave identical results to those obtained in the bottom panel. Data are representative of similar results obtained in three preparations.

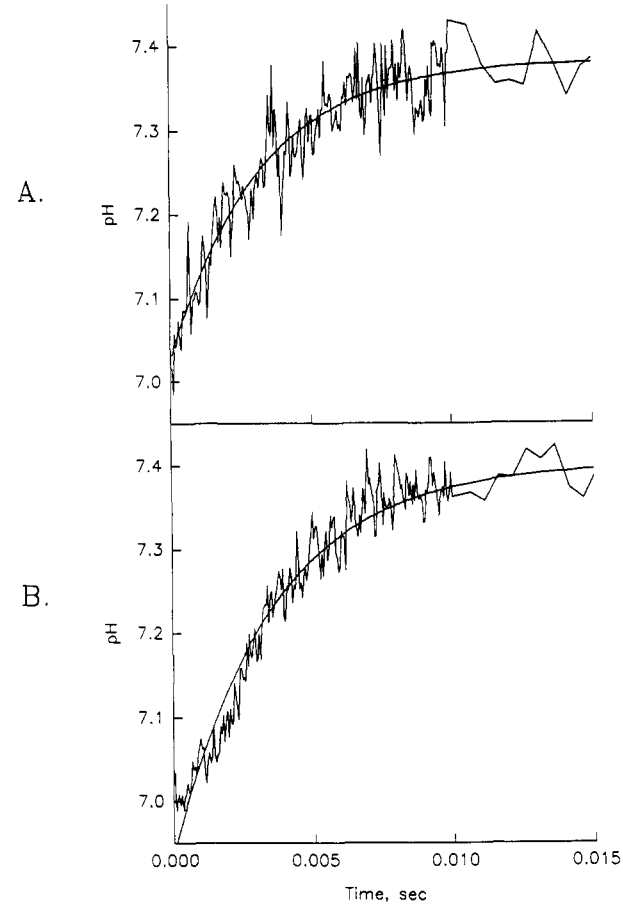

FIGURE 8: Comparison of NH_3 flux into liposomes and CHIP proteoliposomes. Control liposomes (A) or CHIP proteoliposomes (B) pre-equilibrated to pH 7.0 were abruptly exposed to a final extravesicular ammonium/ammonia concentration of 20 mM, and the time course of the resulting alkalinization of intravesicular pH was monitored on the stopped-flow device.

by the presence of other transporters in red cells, including a urea carrier, the glucose transporter, and the Cl^-/HCO_3^- exchanger. Using proteoliposomes in which CHIP is the sole protein, we examined several aspects of the water channel function: structure and orientation of CHIP intramembrane particles, unit water permeability, potential functional importance of specific membrane lipids and the C-terminal domain of CHIP, sensitivities to specific mercurial reagents, and the selectivity of the channel to water over other small charged and uncharged molecules.

These studies revealed several distinct structural features of CHIP in proteoliposomes. CHIP was reconstituted into all proteoliposomes in a preparation, not just a subpopulation. Reconstituted CHIP was oriented in both directions, and the 24-kDa proteolytically cleaved form of CHIP exhibited the properties of the native molecule. CHIP mutants in which the 4-kDa C-terminal domain is missing are not active when expressed in *X. laevis* oocytes (Jung, Preston, and Agre, unpublished observation). Although the functions of the C-terminal domain were not investigated directly, a role in membrane targeting is suspected, since the distribution of charged residues is similar among CHIP and related proteins (Preston & Agre, 1991; Fushimi et al., 1993). The potential functional importance of specific lipids was not observed, although the existence of an annulus of tightly bound, essential lipid cannot be excluded, despite the fact that no labeling of CHIP was observed when red cells were incubated with [^{3}H]-palmitic, -myristic, or -oleic acids (Hartel-Schenk & Agre, 1992). Therefore, the large water conductance and selectivity of CHIP are most likely determined by the protein structure alone.

Reconstituted CHIP formed intramembrane particles which were evenly distributed at reconstitution densities corresponding to 1×, 2.5×, and 5× the density of CHIP within native red cells. The P_f correlated directly with CHIP density, permitting a refined calculation of the unit conductance and suggesting that cooperativity is not involved. It remains uncertain why the relationship between the number of intramembranous particles per vesicle and CHIP density was somewhat less than linear. The observations are consistent with CHIP being organized as tetramers, but when reconstituted at higher densities, CHIP may exist as tetramers plus some octamers. Although it is possible that perturbation of the oligomeric structure of CHIP into either monomeric subunits or non-naturally occurring high molecular weight complexes may have occurred during sample preparations, the calculations from freeze–fracture morphometry are reasonably consistent with previous sedimentation analyses, which failed to reveal the presence of any CHIP in the fractions corresponding to monomeric subunits (approximately 2 S)

but contained a single major peak running at 5.7 S. The sedimentation coefficient and Stokes radius determination provided a calculated molecular weight of approximately 190 kDa, which converted to 135 kDa when corrected for detergent binding (Smith & Agre, 1991). The apparent lack of dynamic equilibrium between monomers and oligomeric complexes precludes direct evaluation of the role of structural assembly in water permeability. Thus, we are left without a molecular explanation for why CHIP is organized as a multisubunit oligomer but is comprised of subunits which may be independently functional units when assessed by radiation inactivation (van Hoek et al., 1991) or coexpression of site-directed mutants (Preston et al., 1993).

Several studies have provided insight into the aqueous pathway through the CHIP molecule. The reversible inhibition by mercurials is due to a single mercury-sensitive site at Cys-189 (Preston et al., 1993). Here it is shown that all characteristics of the mercury inhibition of red cell and renal proximal tubule water channels are reproduced by proteoliposomes containing only CHIP. The limited accessibility to this residue in the defined system is consistent with the prevailing notion that the mercury site lies near a narrowing of the pore, thereby only permitting passage of water, but not molecules such as NH_3 which are only slightly larger. Although the residues lining the aqueous pathway have not yet been delineated, the lack of permeability by ions suggests that charged residues may exist within or nearby, serving as repellants to charged molecules.

The CHIP proteoliposomes described recently (Zeidel, et al., 1992) and in this report will permit high-resolution biophysical analyses which were not previously possible. For example, determination of CHIP-mediated diffusional permeability by NMR may now be feasible. Overexpression in oocytes has permitted considerable insight into the function of CHIP; however, only a small fraction of the overexpressed proteins are present at the oocyte surface. Therefore low P_f values of site-directed mutant forms of CHIP may result from maldistributions of the protein rather than a true reduction in water permeability. This may now be overcome by expressing CHIP and mutant forms of CHIP in cell free systems, purifying the protein by the simple methods reported here, followed by reconstitution of the protein into proteoliposomes. This approach may also be used for characterization of CHIP from red cells of certain clinical states, such as sickle cell anemia, where cell dehydration is known to occur. Finally, the propensity of CHIP to reconstitute efficiently into synthetic lipid membranes indicates that preparation of two dimensional crystals will be a feasible method of defining the shape of the molecule (Walz et al., 1994).

ADDED IN PROOF

While this manuscript was in press, a freeze–fracture study of CHIP was published by other investigators (Verbavatz et al., 1993).

REFERENCES

Agre, P., Sasaki, S., & Chrispeels, M. (1993) *Am. J. Physiol. 265*, F461.

Ambudkar, S. V., & Maloney, P. C. (1986a) *Methods Enzymol. 125*, 558–563.

Ambudkar, S. V., & Maloney, P. C. (1986b) *J. Biol. Chem. 261*, 10079–10086.

Benga, G. (1989) In *Water transport in Biological Membranes*, Vol. II, pp 41–62 CRC Press, Boca Raton.

Bennett, V. (1983) *Methods Enzymol. 96*, 313–324.

Chen, C.-C., & Wilson, T. H. (1984) *J. Biol. Chem. 259*, 10150–10158.

Chen, C.-C., Kurokawa, T., Shaw, S.-Y., Tillotson, L. G., Kalled, S., & Isselbacher, K. J.; (1986) *Proc. Natl. Acad. Sci. U.S.A. 83*, 2652–2656.

Dempster, J. A., van Hoek, A. N., de Jong, M. D., & van Os, C. H. (1991) *Pfluegers Arch. Eur. J. Physiol. 419*, 249–254.

Denker, B. M., Smith, B. L., Kuhajda, F. P., & Agre, P. (1988) *J. Biol. Chem. 263*, 15634–15642.

Echevarria, M., Frindt, G., Preston, G. M., Milanovic, S., Agre, P., Fischbarg, J., & Windhager, E. E. (1993) *J. Gen. Physiol. 101*, 827–841.

Finkelstein, A. (1987) *Water movement through lipid bilayers, pores, and plasma membranes, theory and reality*. John Wiley and Sons, New York.

Fischbarg, J., Kuang, K., Vera, J. C., Arant, S., Silverstein, S. C., Loike, J., & Rosen, O. M. (1990) *Proc. Natl. Acad. Sci. U.S.A. 87*, 3244–3247.

Fushimi, K., Uchida, S., Hara, Y., Hirata, Y., Marumo, F., & Sasaki, S. (1993) *Nature 361*, 549–552.

Goldstein, D. A., & Solomon, A. K. (1960) *J. Gen. Physiol. 44*, 1–22.

Grossman, E. B., Harris, H. W., Star, R., & Zeidel, M. L. (1992) *Am. J. Physiol. Cell. 262*, C1109–C1118.

Grunze, M., Forst, B., & Deuticke, B. (1980) *Biochim. Biophys. Acta 600*, 860–869.

Harris, H. W., Kikeri, D., Janoshazi, A., Solomon, A. K., & Zeidel, M. L. (1990) *Am. J. Physiol. 259*, F366–F371.

Harris, H. W., Strange, K., & Zeidel, M. L. (1991) *J. Clin. Invest. 88*, 1–8.

Hartel-Schenk, S., & Agre, P. (1992) *J. Biol. Chem. 267*, 5569–5574.

Laemmli, U. K. (1970) *Nature 227*, 680–685.

Lukacovic, M. F., Verkman, A. S., Dix, J. A., & Solomon, A. K. (1984) *Biochim. Biophys. Acta 778*, 253–261.

Macey, R. I. (1984) *Am. J. Physiol. 246*, C195–C203.

Maloney, P. C., & Ambudkar, S. V. (1989) *Arch. Biochem. Biophys. 269*, 1–10.

Maunsbach, A. B., & Reinholt, F. P. (1992) *Micron Microscopia Acta 23*, 109–110.

Maunsbach, A. B., Skriver, E. S., & Jorgensen, P. L. (1988) *Methods Enzymol. 156*, 430–441.

Maurel, C., Reizer, J., Schroeder, J. I., & Chrispeels, M. (1993) *EMBO J. 12*, 2241–2247.

Moon, C., Preston, G. M., Griffin, C. A., Jabs, E. W., & Agre, P. (1993) *J. Biol. Chem. 268*, 15772–15778.

Nielsen, S., Smith, B. L., Christensen, E. I., Knepper, M. A., & Agre, P. (1993a) *J. Cell Biol. 120*, 371–383.

Nielsen, S., Smith, B. L., Christensen, E. I., & Agre, P. (1993b) *Proc. Natl. Acad. Sci. U.S.A. 90*, 7275–7279.

Preston, G. M., & Agre, P. (1991) *Proc. Natl. Acad. Sci. U.S.A. 88*, 11110–11114.

Preston, G. M., Carroll, T. P., Guggino, W. B., & Agre, P. (1992) *Science 256*, 385–387.

Preston, G. M., Jung, J. S., Guggino, W. B., & Agre, P. (1993) *J. Biol. Chem. 268*, 17–20.

Priver, N., Rabon, E. C., & Zeidel, M. L. (1993) *Biochemistry 32*, 2459–2468.

Sabolic, I., Valenti, G., Verbavatz, J-M., Van Hoek, A. N., Verkman, A. S., Ausiello, D. A., & Brown, D. (1992) *Am. J. Physiol. 263*, C1225–C1233.

Sinensky, M., Pinkerton, F., Sutherland, E., & Simon, F. R. (1979) *Proc. Natl. Acad. Sci. U.S.A. 76*, 4893–4897.

Skriver, E., Maunsbach, A. B., & Jorgensen, P. L. (1980) *J. Cell Biol. 86*, 746–754.

Smith, B. L., & Agre, P. (1991) *J. Biol. Chem. 266*, 6407–6415.

Solomon, A. K., Chasan, B., Dix, J. A., Lukacovic, M. F., Toon, M. R., & Verkman, A. S. (1983) *Ann. N.Y. Acad. Sci. 414*, 97–124.

van Hoek, A. N., Hom, M. L., Luthjens, L. H., de Jong, M. D., Dempster, J. A., & van Os, C. H. (1991) *J. Biol. Chem. 266*, 16633–16635.

van Hoek, A. N., & Verkman, A. S. (1992) *J. Biol. Chem. 267*, 18267–18269.
Verbavatz, J. M., Brown, D., Sabolic, I., Valenti, G., Ausiello, D. A., Van Hoek, A. N., Ma, T., & Verkman, A. S. (1993) *J. Cell Biol. 123*, 605–618.
Verkman, A. S. (1989) *Am. J. Physiol. 257*, C837–C850.
Walz, T., Smith, B. L., Zeidel, M. L., Engel, A., & Agre, P. (1994) *J. Biol. Chem. 269*, 1583–1586.
Ye, R., & Verkman, A. S. (1989) *Biochemistry 28*, 824–829.
Zeidel, M. L., Albalak, A., Grossman, E. B., & Carruthers, A. (1992a) *Biochemistry 31*, 589–596.
Zeidel, M. L., Ambudkar, S. V., Smith, B. L., & Agre, P. (1992b) *Biochemistry 31*, 7436–7440.
Zhang, R., Alper, S. L., Thorens, B., & Verkman, A. S. (1991) *J. Clin. Invest. 88*, 1553–1557.
Zhang, R., Skach, W., Hasegawa, H., Van Hoek, A. N., & Verkman, A. S. (1993) *J. Cell Biol. 120*, 359–369.